7th Bangladesh Conference on Industrial Engineering and Operations Management
December 21-22, 2024
Publisher: IEOM Society International, USA DOI: 10.46254/BA07.20240077
Published: December 21, 2024

A Comparison Study of Vehicle's Electro-Hydraulic (EHPS), Electric (EPS) and Hydraulic (HPS) Power Steering System

Robin Barua and Md. Mizanur Rahman
Department of Electrical and Electronic Engineering
Institute of Energy Technology
Chittagong University of Engineering and Technology (CUET),
Chattogram, Bangladesh
robi5374@gmail.com, mizanurr340@gmail.com

Rasel Sen and Saswata Dutta
Department of Electrical and Electronic Engineering
Premier University, Chattogram, Bangladesh
rasel.sen.eee@gmail.com, saswata.an2@gmail.com

Md. Tazul Islam and Syed Masrur Ahmmad
Department of Mechanical Engineering
Chittagong University of Engineering and Technology (CUET),
Chattogram, Bangladesh
tazul2003@cuet.ac.bd, masrur@cuet.ac.bd

Abstract

The aim of this study is to calculate the energy efficiency of an electro-hydraulic power steering system (EHPS), as electric power steering (EPS) system also can be an energy savings solution instead of traditional hydraulic power steering (HPS) system. EHPS consist of electrical, mechanical steering system and hydraulic system. It is an approach to minimize the energy consumption and improve the steering feel of the power steering system of a vehicle. We have developed an electro-hydraulic power steering system and designed a fuzzy-pid controller that can follow the command motor speed. We have calculated, the available motor shaft power to hydraulic efficiency is 53.03%. The mechanical loss includes hydraulics and, rack and pinion loss. This study also focuses on comparison of electro-hydraulic (EHPS), hydraulic power steering (HPS) and electric power steering (EPS) system.

Keywords

EHPS, HPS, EPS, Motor Speed Control, Energy Efficiency and Energy Conversion.

1. Introduction

In electro-hydraulic power steering (EHPS) systems, the primary energy source is the vehicle's battery, which supplies electrical power that is subsequently converted into hydraulic power. Therefore, an analysis of electric power consumption and conversion efficiency is essential for designing an energy-efficient power steering system. Electric power consumption varies depending on the vehicle's weight. For heavier vehicles, the front axle load is greater than that of medium-weight vehicles, resulting in higher electric power consumption. As power consumption increases, the

required battery size (Wh) also increases. In conventional hydraulic power steering (HPS) systems, pressure control is purely hydro-mechanical (Dell'Amico, 2015). In a power steering system, the boost curve is defined by the assistive pressure corresponding to a given torsion bar torque. Steering torque controls the flow rate to the left or right piston by adjusting the orifice size in the rotary valve. The power consumption of the system depends on both vehicle speed and steering torque. In conventional systems, power consumption increases with higher steering torque at a constant vehicle speed, or with higher vehicle speed at constant steering torque. In contrast, in energy-efficient EHPS systems, hydraulic pressure can be regulated, allowing electric power consumption to be adjusted according to vehicle speed by controlling the flow rate of the DC motor pump. The DC motor serves as the main power source in the EHPS system, with motor speed controlled by a microcontroller based on vehicle speed and steering rate. Additionally, a torsion bar inside the steering column regulates the flow rate to the piston (Nimbarte 2013). In these systems, the hydraulic power generated by the vane pump determines both power consumption and steering feel (Sun 2011). This approach enhances both energy efficiency and steering performance in modern vehicles.

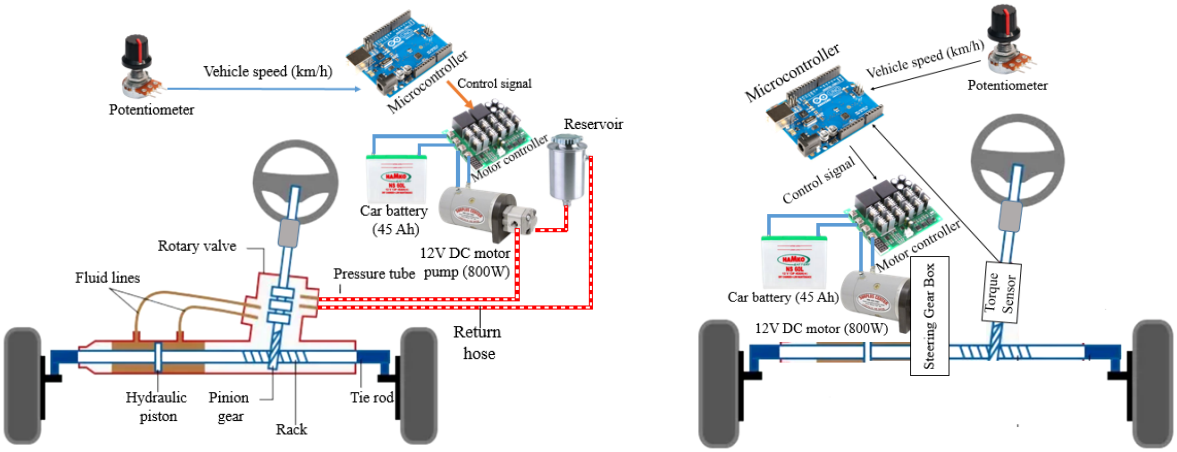

Figure 1. (a) Electro-Hydraulic Power Steering System (EHPS), (b) EPS (Electric Power Steering)

The energy-efficient electro-hydraulic power steering system is depicted in Figure 1(a). This system integrates electrical, hydraulic, and mechanical components. The electrical components include a DC motor pump, motor controller, microcontroller (Arduino Uno), car battery (45 Ah), electric cables, and a potentiometer. The hydraulic components consist of a rack and pinion mechanism with a hydraulic piston, hoses, a reservoir, and the DC motor pump. The mechanical components include the tie rod, steering wheel, rotary valve, steering arm, and related elements. In contrast, an electric power steering (EPS) system, illustrated in Figure 1(b), consists solely of an electric motor and a steering gearbox. An electronic control unit (ECU) regulates the motor speed based on the steering torque. Unlike the electro-hydraulic system, the EPS system does not incorporate hydraulic components. Instead, electrical power is directly converted into mechanical power through the steering gearbox.

1.1 Objectives

Energy conversion efficiency is a critical consideration in the design of power steering systems. With the continuous development of techniques to enhance energy savings, evaluating the energy conversion efficiency of different systems helps manufacturers and customers select the most suitable option for specific vehicles. Power steering systems, such as Electro-Hydraulic Power Steering (EHPS), Hydraulic Power Steering (HPS), and Electric Power Steering (EPS), can all be implemented in vehicles.

The objectives of this study are:

1. Experimental design and motor speed control of EHPS,
2. Calculation of the energy conversion efficiency of EHPS,
3. Comparative analysis and discussion of EHPS, EPS, and HPS.

2. Literature Review

For automobiles equipped with a 42 V DC supply, an electric-driven pump unit was developed for the EHPS system, powered by an interior-type synchronous motor (Rhyu 2017). Motor speed control plays a crucial role in the performance of the EHPS system. A fuzzy-PID control strategy was implemented to regulate the speed of a brushless

DC motor (Dong, 2018), enabling smooth speed control under varying load conditions. The motor speed was increased beyond its nominal speed using the field-weakening method. In another study, an induction motor control strategy was simulated for EHPS, demonstrating effective control performance (Lin and Wang). A control method for brushless DC motors in hydraulic-electric power steering systems was developed to improve steering feel while conserving energy (Fujita, 2001). An Electric Power Steering (EPS) system was implemented on a light commercial vehicle, utilizing a brushless DC motor to control torque and provide an enhanced steering feel. The motor was directly connected to the recirculating ball gear (Murugan, 2008). To minimize power consumption at high vehicle speeds, an electromagnetic clutch was used to disengage the vane pump supply (Sonchal, 2012). Although these techniques aim to reduce power consumption, the electric power consumption itself has not been thoroughly analyzed. The key parameters influencing energy efficiency such as voltage, current, vehicle speed, and motor speed remain inadequately addressed in the literature.

3. Experimental Test Bench

Figure 2 shows the electro-hydraulic power steering (EHPS) system developed in our laboratory. A pressure gauge has been installed in the pressure line to monitor system pressure. The motor controller is enclosed within the controller box, and a potentiometer is used to simulate vehicle speed (km/h) as input. The mechanical steering system, based on the Ackerman steering geometry, is securely fixed to the ground. All hydraulic components have been properly sealed to system function properly. The system operates under no-load conditions on the front wheels. Steering torque (Nm) is calculated using a weight scale. Applying force to the steering wheel increases system pressure (bar), which in turn raises the load current. Measurements of steering torque and load current have been recorded to evaluate system performance.

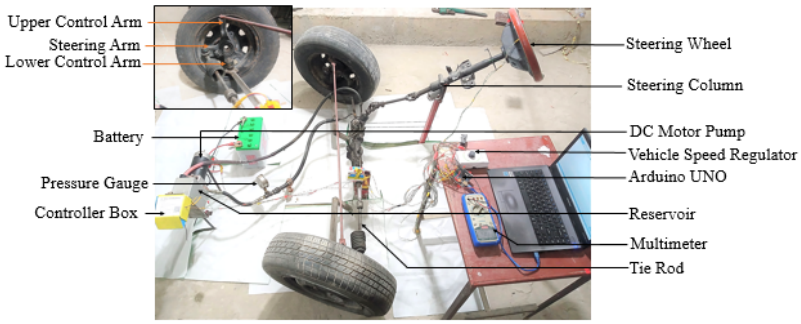

Figure 2. Experimental Test Bench of EHPS

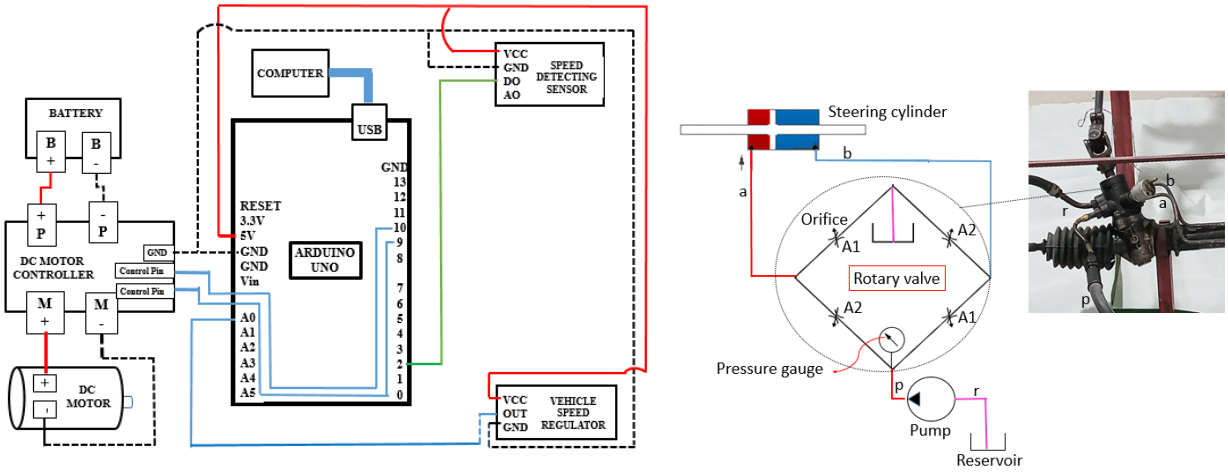

Figure 3. (a) Electrical Circuit Diagram, and (b) Hydraulic circuit diagram

The electrical circuit diagram is shown in Figure 3(a). The microcontroller, Arduino UNO, is connected to a PC for code uploading and data streaming. The Excel Data Streamer feature is used to read and save real-time data. A modified DC motor controller is used, which can be controlled via the Arduino. The motor has two control pins,

allowing it to run in a clockwise direction. The direction of the road wheel changes according to the rotary valve (Barua, 2022).

Figure 3(b) shows the hydraulic circuit of the system. In the neutral position, when no steering torque is applied, the fluid is distributed equally through orifices 'A1' and 'A2' to the pressure chambers 'a' and 'b,' as well as to the reservoir. When steering torque is applied, a hydraulic pressure difference is created between the chambers. As hydraulic pressure builds, the motor speed tends to decrease. However, the fuzzy-PID controller detects this change and maintains the motor speed at the set point by increasing the voltage. Conversely, when steering torque is reduced, the hydraulic pressure drops, and the motor speed tends to increase. The fuzzy-PID controller detects this situation and adjusts the voltage to decrease the motor speed, maintaining the set point. The cross-sectional area of the hydraulic piston is 31.4 m².

4. Methodology

The parameters to measure electric and hydraulic power are current, voltage, flow rate, and pressure. Table 1 shows the parameter measurement table.The motor speed is measured using an IR speed sensor, as shown in Figure 4(a). When the encoder card passes through the IR sensor, the signal is processed by the Arduino microcontroller to calculate the motor speed. The flow rate is then calculated based on the motor speed. It has been tested that at 5340 rpm, the flow rate is 2 lpm. The interval between the motor speed measurement and the voltage drop measurement by the Arduino does not affect the validity of the data.

In the EHPS, the motor speed automatically adjusts based on vehicle speed. Since no vehicle engine is available, a potentiometer is used as the vehicle speed input, as shown in Figure 4(b). The analog input (0–1023) from the potentiometer is mapped to vehicle speed (0–120 km/h). By adjusting the potentiometer knob, we can send the vehicle speed signal to the Arduino.he actual system does not include a pressure gauge. To measure hydraulic pressure, a pressure gauge has been installed in the pressure line, as shown in Figure 4(c).

Table 1. Equations for measuring parameters

Parameters	Equation
Vehicle speed, x (km/h)	Potentiometer Output Mapping (0-1023) to (0-120 km/h)
Motor speed (rps)	IR Sensor Reading
Motor speed setpoint, y	45-0.2x
Flow rate,Q (lpm)	$\frac{motor\ rpm * 2\ lpm}{5340\ rpm}$ [At 5340 rpm, 2 lpm flow rate]
Pressure, P (bar)	Pressure Gauge
Battery voltage, $V_{battery}$ (V)	Voltmeter (12 V)
PWM Output (Arduino)	0-255
PWM Voltage, V_{pwm}	$\frac{pwm\ output * V_{battery}}{255}$
Shunt voltage, V_{sh} (mV)	Voltmeter Reading (mV)
Current, I (A)	$\frac{V_{sh} * 50A}{75\ mV}$ [At 75mV, 50A current]
Electric Power, P_{in} (W)	V_{pwm}*I
No Load Electric Power, P_0(W)	V_0*I_0
Load Power, $P_{5.23}$ (W)	$V_{5.23}$*$I_{5.23}$
Hydraulic power, P_{out} (W)	$\frac{P * Q}{0.6}$
Mechanical loss, P_{mech} (W)	$P_{5.23}$-P_0-P_{out}
Steering Torque (Nm)	9.8N *meter scale reading

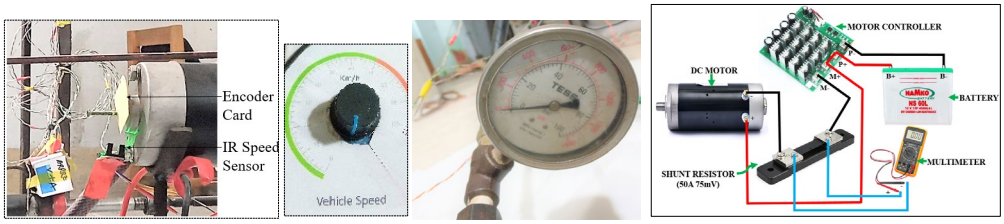

(a) (b) (c) (d)

Figure 4. (a) Motor speed-Encoder, (b) Potentiometer-Vehicle speed, (c) Pressure Gauge, and (d) Current measurement with shunt and multimeter

The current through the motor is the primary source of power consumption in an energy-efficient electro-hydraulic power steering system. In a series circuit, the current remains the same through all components (Tony and John). To measure this, a shunt resistor was connected between the motor and controller on the negative line, and the voltage drop across the shunt resistor was measured using a multimeter, as shown in Figure 4(d). This allows us to determine the current consumption when steering torque is applied.Steering torque was measured by setting the weight scale to achieve a torque of 5.23 Nm. The corresponding current consumption was recorded.

Motor speed, battery supply voltage, and vehicle speed were recorded in Excel using the Data Streamer feature. Current consumption data was also manually recorded using the shunt resistor.
To maintain a constant battery voltage of 12V throughout the test, a charger was employed, as the 45 AH battery could not provide sufficient power for extended periods. This continuous charging simulated the real-time functioning of a vehicle's dynamo, which would typically recharge the battery during use. To begin, it is essential to determine the electrical power generated under different operating conditions, starting with the no-load scenario. Figure 5 presents the power flow diagram, illustrating how electrical energy is converted into mechanical energy by the electric motor. The motor's electric power input (Pin) and the system's hydraulic power output ($Pout$) are determined using the formulas outlined in Table 1. We examine two primary conditions: no-load electric power and full-load electric power. In this setup, the motor converts electrical energy into mechanical power, which is then converted into hydraulic power. The motor controller, placed between the 12V battery and the 800W DC motor, governs this process of energy conversion.

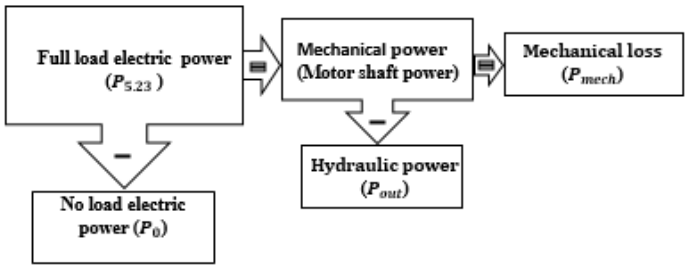

Figure 5. Power-flow diagram of EHPS system

Pulse width modulation (PWM) is an energy-efficient control method commonly used to regulate motor speed. It consumes minimal power to drive the controller's MOSFET, with the majority of the electrical power being used by the motor itself. The no-load electric power (Pn), as measured at 0 Nm steering torque in Table 1, is primarily consumed to circulate fluid within the hydraulic circuit, without generating hydraulic pressure. In contrast, the full-load electric power corresponds to the hydraulic power generated when hydraulic pressure is produced at 5.23 Nm torque. The difference between the full-load and no-load electric power represents the mechanical power, which is then converted into hydraulic power by the hydraulic pump. Mechanical losses ($Pmech$) include losses from both the hydraulic pump and the hydraulic circuit components.

4) We have observed the relationship between steering torque and hydraulic pressure, as shown in Table 2. In the absence of a controller, we applied a full 12V power supply to the motor and observed that the motor speed was 90 rps at 0

Nm steering torque. As the steering torque was increased, the hydraulic pressure also rose. Consequently, the motor speed decreased due to the higher load. To solve this issue, we implemented a fuzzy-PID controller to regulate motor speed in nonlinear operating conditions, ensuring more stable performance across varying loads.

Table 2. Torque vs. Hydraulic Pressure vs. Motor Speed

Torque (Nm)	**Pressure (bar)**	**Motor Speed**
0	0	90 rps
2.75	5	89 rps
2.94	8	88 rps
3.24	12	87 rps
3.73	22	86 rps
4.23	28	82 rps
4.51	32	81 rps
4.71	35	80 rps
5.00	37	79 rps
5.20	40	78 rps

Fuzzy-PID Control:

We initially selected the PID controller to achieve and maintain the motor speed at its set value. The Arduino PID_v1 library was used, along with its automatic mode. The values for the proportional (k_p), derivative (k_d), and integral (k_i) gains were set to 0.1, 0.09, and 1, respectively. To ensure the motor reaches its set point speed quickly, we adjusted the proportional and derivative gains using a fuzzy algorithm. In this fuzzy adaptive PID control, there is one input variable and two output variables. The input variable is speed error, while the output variables are k_p and k_i. The speed error is defined by seven triangular membership functions: enl, enm, ens, eze, eps, epm, and epl. The membership functions for the output variables k_p include kpsm, kpmd, and kpbg, while for k_i, they are kism, kimd, and kibg. The ranges and seven rules are provided in Table 3.

Table 3. Range and Rules of Membership Function

<table>
<tr><th>Input (Speed error)</th><th>Output (k_p)</th><th>Output(k_i)</th></tr>
<tr><td>enl (-90, -67.5, -67.5, -45)</td><td>kpsm (1, 2, 2, 3)</td><td>kism (1, 2, 2, 3)</td></tr>
<tr><td>enm (-67.5, -45, -45, -22.5)</td><td>kpmd (2, 3, 3, 4)</td><td>kimd (2, 3, 3, 4)</td></tr>
<tr><td>ens (-45, -22.5, -22.5, 0)</td><td>kpbg (3, 4, 4, 5)</td><td>kibg (3, 4, 4, 5)</td></tr>
<tr><td>eze (-22.5, 0, 0, 22.5)</td><td colspan="2" rowspan="4">Rule:
If error is epl then kpsm and kism.
If error is epm, then kpmd and kimd.
If error is eps, then kpbg and kibg.
If error is ens, then kpbg and kibg.
If error is enm, then kpmd and kimd.
If error is enl, then kpmd and kimd.
If error is eze, then kpsm and kism.</td></tr>
<tr><td>eps (0, 22.5, 22.5, 45)</td></tr>
<tr><td>epm (22.5, 45, 45, 67.5)</td></tr>
<tr><td>epl (45, 67.5, 67.5, 90)</td></tr>
</table>

5.1 Result and Analysis

In this system, we have set the motor speed set point so that it decreases with increasing vehicle speed. So, if vehicle speed increases, the controller can decrease the motor speed using the fuzzy-PID control algorithm. The motor keeps running even if no steering occurs, as we have not used a steering torque or steering angle sensor. In addition, it takes more time from motor off state to set point speed than set point to set point speed.

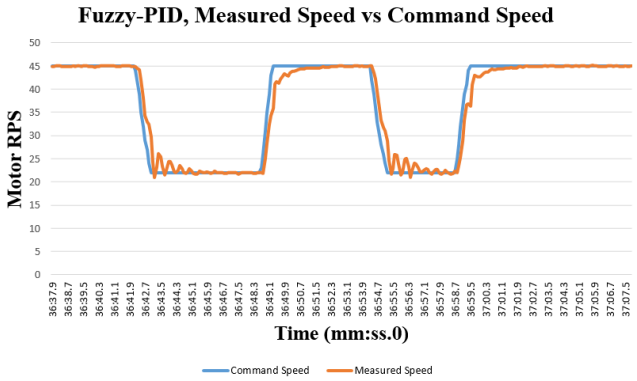

Figure 6. Measured speed vs command speed

In Figure 6, the blue smooth line represents the motor speed setpoint, which is the command motor speed by the microcontroller, while the yellow line represents the measured speed, or the actual motor speed. At time 37.9, the vehicle speed was zero. At time 41.9, we increased the vehicle speed to 120 km/h by adjusting the knob. According to Equation (Row,3) in Table 1, the new setpoint becomes 21 rps, which the fuzzy-PID controller maintains. After some fluctuations, at time 45.9, the speed stabilizes. At time 49.1, the vehicle speed is reduced to 0 km/h, which results in a new motor speed of 45 rps. By time 51.5, the fuzzy-PID controller adjusts and reaches the new motor speed setpoint. This demonstrates that the measured speed closely follows the command speed.

Table 4. Electric Power at Different Vehicle Speed and Motor Speed of EHPS at Torque=0 Nm and 5.23 Nm

Vehicle speed (km/h)	**Motor Speed** (RPS)	**Torque=0 Nm**			**Torque= 5 Nm**		
		Voltage V_0 (V)	**Current** I_0(A)	**Power** P_0 (W)	**Voltage** $V_{5.23}$ (V)	**Current** $I_{5.23}$ (A)	**Power** $P_{5.23}$ (W)
0	45	4.65	17.46	81.189	5.5	23.5	129.25
5	44	4.58	17.18	78.6844	5.38	22.9	123.202
10	43	4.5	16.9	76.05	5.27	22.4	118.048
15	42	4.43	16.62	73.6266	5.18	22.1	114.478
20	41	4.35	16.34	71.079	5.1	21.7	110.67
25	40	4.28	16.06	68.7368	5	21.3	106.5
30	39	4.19	15.73	65.9087	4.96	20.8	103.168
35	38	4.11	15.4	63.294	4.79	20.4	97.716
40	37	4.02	15.06	60.5412	4.65	19.8	92.07
45	36	3.94	14.73	58.0362	4.5	19.5	87.75
50	35	3.85	14.4	55.44	4.4	19	83.6
55	34	3.78	14.1	53.298	4.4	18.5	81.4
60	33	3.7	13.81	51.097	4.3	18.2	78.26
65	32	3.63	13.52	49.0776	4.17	17.8	74.226
70	31	3.55	13.22	46.931	4.09	17.4	71.166
75	30	3.48	12.93	44.9964	4.1	17	69.7
80	29	3.39	12.62	42.7818	3.96	16.7	66.132
85	28	3.31	12.32	40.7792	3.84	16.3	62.592
90	27	3.22	12.01	38.6722	3.76	15.8	59.408
95	26	3.14	11.7	36.738	3.64	15.4	56.056
100	25	3.05	11.4	34.77	3.56	15.1	53.756
105	24	3	11.17	33.51	3.45	14.5	50.025
110	23	2.94	10.94	32.1636	3.3	13.8	45.54
115	22	2.88	10.72	30.8736	3.2	13.5	43.2
120	21	2.83	10.49	29.6867	3.1	12.9	39.99

In this system, electric power is converted into hydraulic power. The steering torques applied to the steering wheel are 0 Nm and 5.23 Nm. Table 4 presents the experimental data for electric power, vehicle speed, motor speed, voltage, current, and power at 0 Nm steering torque. At 0 Nm, no hydraulic pressure is developed, and therefore, no electric power is converted into hydraulic power. Table 5 shows the hydraulic power consumption at 5.23 Nm. At this steering torque, the rotary valve opens fully, and the flow rate from the hydraulic pump to the pressure chamber becomes equal.

Table 5. Hydraulic Power at Different Vehicle Speed and Motor Speed of EHPS at Torque=5.23 Nm

Vehicle speed (km/h)	**Motor Speed** (RPS)	**Pressure** (bar)	**Flow rate** (lpm)	**Power** (W)
0	45	15.1	1.012809	25.48903
5	44	14.8	0.993258	24.50037
10	43	14.4	0.966292	23.19101
15	42	14	0.945618	22.06442
20	41	13.9	0.942247	21.82873
25	40	13.4	0.900674	20.11
30	39	13	0.878652	19.03
35	38	12.8	0.861124	18.37
40	37	12.6	0.839101	17.62
45	36	12.4	0.809438	16.72
50	35	12.2	0.791011	16.08
55	34	11.9	0.764944	15.17
60	33	11.5	0.743596	14.25
65	32	11	0.721348	13.22
70	31	10.8	0.717303	12.91
75	30	10.3	0.681573	11.70
80	29	10	0.665843	11.09
85	28	9.6	0.638652	10.21
90	27	9.2	0.616629	9.45
95	26	8.6	0.594607	8.52
100	25	8	0.566742	7.55
105	24	7.6	0.54809	6.94
110	23	6.9	0.529663	6.09
115	22	6	0.500674	5.00
120	21	5	0.482247	4.01

Table 6. Power Conversion Efficiency Calculation

Motor Speed (RPS)	No Load Electric Power P_0 (W)	Full Load Power $P_{5.23}$ (W)	Mechanical Input Power ($P_{5.23} - P_0$), (W)	Hydraulic Power, $P_{out}(W)$	Mechanical Loss, P_{mech}(W)
45	81.189	129.25	48.06	25.48 W	22.58 W
Electric to Hydraulic Efficiency, $\frac{P_{out}}{P_{5.23}}$*100% = **19.72%**			Mechanical to Hydraulic Efficiency, $\frac{P_{out}}{P_{5.23}-P_0}$*100% = **53.02%**		

From Table 6, we observe that at 45 RPS, the no-load electric power consumption is 81.189 W. When a steering torque of 5.23 Nm is applied, the electric power consumption increases to 129.25 W. Therefore, 48.06 W of motor shaft power is converted into hydraulic power. Here, the motor shaft power represents the mechanical output power. The hydraulic power consumption is 25.48903 W, resulting in a mechanical-to-hydraulic power efficiency of

approximately 53%. The overall electric-to-hydraulic efficiency is 19.72%. A heating issue is observed in the motor due to the use of an older hydraulic pump motor set. Replacing it with a new DC motor pump would likely increase the conversion efficiency.

5.2 Comparison of HPS, EHPS and EPS

The same motor can be utilized for the EPS system. In the case of EPS, since there is no hydraulic power, the motor shaft power at 45 rpm with 5.23 Nm of torque is 48.06 W, which can be directly used to drive the steering gear. In the EHPS system, when torque is applied, the rotary valve opens, and the fluid is divided into two paths. The fluid directed to the piston generates the primary hydraulic power required for vehicle steering, while the fluid returned to the reservoir causes a circulation loss. In EPS, this circulation power loss is eliminated, as there are no hydraulic components involved. The hydraulic circuit in both HPS and EHPS is identical, with the HPS system employing a vane pump.

Table 7. Comparison of HPS, EHPS and EPS

Parameters	**HPS**	**EHPS**	**EPS**
Pump	Vane pump	Motor driven pump	No pump
Steering gear	Rack and pinion	Rack and pinion	Rack and pinion
Assist power	Hydraulic	Electro-hydraulic	Electric
Hydraulic circuit	Wheatstone bridge	Wheatstone bridge	No hydraulic circuit
Power source	Vehicle engine	Battery	Battery
Rotary valve	Open center	Open center	No rotary valve
ECU	No ECU	Yes	Yes
Autonomous vehicle	Not suitable	Not suitable	Suitable

Table 7 presents a comparison of different systems based on several key parameters. The EPS system is particularly suitable for electric vehicles, as they are powered by batteries. Vehicles with combustion engines require additional batteries to operate the HPS, EHPS, and EPS systems. Currently, the EPS system is used in autonomous vehicles. Features such as Honda Sensing, Lane Keeping Assist, Lane Tracing Assist, AcuraWatch, and Comma AI can be integrated into vehicles equipped with an EPS system (supported cars). The EHPS system is not suitable for this application, as it depends on a mechanical steering torque mechanism with a torsion bar, which only allows fluid flow when the driver applies force to the steering wheel.

6. Conclusion

The fuzzy-PID controller can effectively track the required motor speed, providing the driver with a good steering feel while saving energy at high vehicle speeds. However, achieving smooth control of the motor speed further enhances the steering feel. Reducing fluctuations in motor speed control can significantly improve steering response. Additionally, the use of a high-efficiency motor and pump will increase overall system efficiency. There is a circulating flow loss in the system, which can be minimized by stopping the motor when it is not needed. To accomplish this, a torque or angle sensor, along with a brushless motor, needs to be integrated. Brushless motors offer faster response times, higher efficiency, and lower heat generation compared to brush motors. On the other hand, the EPS system is particularly well-suited for electric and autonomous vehicles, as well as for lane-keeping assistance. For heavy vehicles, the EHPS system is preferable, as hydraulics provide high power density.

References

Barua, R., Islam, M. T., Ahmmad, S. M., Rana, M. M., Sen, R., Rahman, M. M., Conventional power steering system of vehicle and continuous improvement, International Conference on Mechanical, Industrial and Energy *Engineering*, Khulna, Bangladesh, December 22-24, 2022.

Dong, W., Song, J., Cheng, S., Yu, L. and Lu, X., Speed Control of BLDC Motor in Electro-Hydraulic Power Steering System Based on Fuzzy-PI Controller, SAE Technical Paper 2018-01-0698, 2018.

DellrAmico, A., Krus, P., Modeling, Simulation, and Experimental Investigation of an Electrohydraulic Closed-Center Power Steering System. IEEE/ASME Transactions on Mechatronics, (2015), 1–11. doi:10.1109/TMECH.2014.2384005.

FUJITA, K., Development of Control Methods for Hydraulic-Electric Power Steering System Using Brushless DC Motor, KOYO Engineering Journal English Edition No. 159E (2001).

Lin, Li., Wang, W., Castillo, Liu, Zheng-qi., Modeling and Simulation of Slip Frequency Control for Induction motor in Electric Vehicle EHPS System , Applied Mechanics and Materials, Vols.635-637(2014), pp 1251-1255.

M. R. Nimbarte, L.P. Raut, Efficiency Analysis of Hydraulic Power Steering System, International Journal of Engineering Research and Applications (IJERA), Vol. 3, Issue 3, May-Jun 2013, pp. 1230-1235.

MURUGAN, R., NANDAKUMAR, S., MOHIYADEEN, M S., DSP-based electric power assisted steering using BLDC motor, Sadhana Vol.33, Part 5, October 2008, pp. 581-590, 2018.

Rhyu, S., Kim, Y., Choi, J., Development of an Electric Driven Pump Unit for Elctro-Hydraulic Power Steering of 42V Automobile, IEEE, 2017.

Sonchal, C., Gajankush, J., Kulkarni, A., and Pawar, S., "Energy Efficient Hydraulic Power Assisted Steering System, SAE Technical Paper 2012-01-0976, 2012.

Sun, Y., He, P., Zhang, Y., & Chen, L. , Modeling and Co-simulation of Hydraulic Power Steering System, 2011, Third International Conference on Measuring Technology and Mechatronics Automation, 2, 595-600,2011.

Tony R. Kuphaldt and John Haughery, Book: Applied Industrial Electricity, Chapter3, Circuit topology and laws.

Supported cars, https://github.com/commaai/openpilot/blob/master/docs/CARS.md#dont-see-your-car-here.

Acknowledgement

The authors would like to express their sincere gratitude to Chittagong University of Engineering and Technology (CUET) for providing the necessary laboratory facilities and support throughout the course of this research. Their contribution was invaluable in the successful completion of this work.

Biographies

Robin Barua is currently pursuing a Ph.D. in Electrical and Electronic Engineering at CUET. He completed his M.Sc. in Engineering in Energy Technology at CUET in 2023 and received his B.Sc. in Electrical and Electronic Engineering from Premier University, Chattogram, in 2017. After graduation, he worked as an assistant project engineer for six months at Lucky Automation and Engineering Ltd., gaining practical experience in installing fire detection and protection systems. His research interests include *Control Systems*, *Power Electronics*, and *Electric Vehicles*.

Dr. Md Tazul Islam is a Professor in the Department of Mechanical Engineering at CUET. He earned his B.Sc., M.Sc., and Ph.D. in Mechanical Engineering from Bangladesh University of Engineering and Technology (BUET). His research interests encompass *Fluid Mechanics and Machinery*, *Renewable Energy and Refrigeration*, and *Air Conditioning*. He has expertise in hydrodynamics, experimental fluid mechanics, and aerodynamics.

Syed Masrur Ahmmad is an Associate Professor in the Department of Mechanical Engineering at CUET. He holds a B.Sc. in Mechanical Engineering from CUET and an M.Sc. in Mechatronics Engineering from the International Islamic University Malaysia (IIUM). His research interests include *Mechatronics* (control and robotics), *Applied Mechanics*, and *Automobile Engineering*. He specializes in design engineering.

Md. Mizanur Rahman completed his M.Sc. in Engineering in Energy Technology at CUET in 2023. He earned his B.Sc. in Electrical and Electronic Engineering from the University of Information Technology and Sciences (UITS), Bangladesh, in 2015. His research interests focus on *Energy Saving Techniques*, *AI*, and the *Internet of Things*.

Rasel Sen earned his B.Sc. in Electrical and Electronic Engineering from Premier University, Chattogram, in 2017. After graduation, he worked for one year as an assistant project engineer at Lucky Automation and Engineering Ltd., where he gained practical experience in installing fire detection and protection systems. His research interests include *Renewable Energy* and *Smart Grid Systems*.

Saswata Dutta received his B.Sc. in Electrical and Electronic Engineering from Premier University, Chattogram, in 2017. He worked as an assistant project engineer for one year at Lucky Automation and Engineering Ltd., where he gained practical experience in installing fire detection and protection systems. His research interests include *Control Systems*, *Automation*, and *Electric Vehicles*.